



1 **A Hydrological Emulator for Global Applications**

2 Yaling Liu<sup>1</sup>, Mohamad Hejazi<sup>1</sup>, Hongyi Li<sup>2</sup>, Xuesong Zhang<sup>1</sup>, Guoyong Leng<sup>1</sup>

3 <sup>1</sup>Joint Global Change Research Institute, Pacific Northwest National Laboratory, 5825

4 University Research Court, College Park, Maryland 20740, United States

5

6 <sup>2</sup>Department of Land Resources and Environmental Sciences, Montana State University,

7 Bozeman, MT 59717, United States

8

9 Correspondence to: Yaling Liu ([cauliuyaling@gmail.com](mailto:cauliuyaling@gmail.com))



10 **Abstract**

11 While global hydrological models (GHMs) are very useful in exploring water resources and  
12 interactions between the Earth and human systems, their use often requires numerous model  
13 inputs, complex model calibration, and high computation costs. To overcome these challenges,  
14 we construct an efficient open-source and ready-to-use hydrologic emulator (HE) that can mimic  
15 complex GHMs at a range of spatial scales (e.g., basin, region, globe). We constructed both a  
16 lumped and a distributed scheme of the HE based on the monthly “*abcd*” model, for users’  
17 choice – minimal computational cost with reasonable model fidelity, or heavier computational  
18 load with better predictability. Model predictability and computational efficiency were evaluated  
19 in simulating global runoff from 1971-2010 with both the lumped and distributed schemes. The  
20 results are compared against the runoff product from the widely-used Variable Infiltration  
21 Capacity (VIC) model. Our evaluation indicates that the lumped and distributed schemes present  
22 comparable results regarding annual total quantity, spatial pattern and temporal variation of the  
23 major water fluxes (e.g., total runoff, evapotranspiration) across the global 235 basins (e.g.,  
24 correlation coefficient  $r$  between the annual total runoff from either of these two schemes and the  
25 VIC is  $>0.96$ ), except for several cold (e.g., Arctic, Interior Tibet), dry (e.g., North Africa ) and  
26 mountainous (e.g., Argentina) regions. Compared against the monthly total runoff product from  
27 the VIC (aggregated from daily runoff), the global mean Kling-Gupta efficiencies are 0.75 and  
28 0.79 for the lumped and distributed schemes, respectively, with the distributed one better  
29 capturing spatial heterogeneity. Notably, the computation efficiency of the lumped scheme is two  
30 orders of magnitude higher than the distributed one, and seven orders more efficient than the  
31 VIC model. Our results suggest that the revised lumped “*abcd*” model can serve as an efficient



32 and acceptable HE for complex GHMs and is suitable for broad practical use, and the distributed  
33 scheme is also an efficient alternative if spatial heterogeneity is of more interest.



## 34 **1 Introduction**

35           A global hydrological model (GHM) is an effective tool to understand how water moves  
36 between soil, plants and the atmosphere. In terms of spatial discretization, hydrological models  
37 can be classified into: 1) lumped models treating one basin as a homogeneous whole and  
38 disregarding spatial variations, such as the Sacramento Soil Moisture Accounting Model  
39 (Burnash et al., 1973); and 2) distributed models where the entire basin is divided into small  
40 spatial units (e.g., square cells or triangulated irregular network) to capture spatial variability,  
41 such as the PCRaster Global Water Balance (Van Beek and Bierkens, 2009) and the WASMOD-  
42 M (Widén-Nilsson et al., 2007). For simplicity, models with division of one basin into separate  
43 areas or sub-basins are also categorized as distributed ones here. The corresponding  
44 predictability and computational efficiency of GHMs may vary from model to model, due to  
45 difference in complexity and structure. Recent years have seen rapid progress in GHMs. They  
46 are widely used in assessing the impacts of climate change and land surface changes on the water  
47 cycle (Alcamo and Henrichs, 2002; Arnell and Gosling, 2013; Liu et al., 2013; Liu et al., 2014;  
48 Nijssen et al., 2001a), exploring spatial and temporal distribution of water resources (Abdulla et  
49 al., 1996; Alkama et al., 2010; Bierkens and Van Beek, 2009; Gerten et al., 2005; Tang et al.,  
50 2010), examining how human activities alter water demand and water resources (De Graaf et al.,  
51 2014; Döll et al., 2009; Hanasaki et al., 2008; Liu et al., 2015; Rost et al., 2008; Vörösmarty et  
52 al., 2000), and investigating the interactions between human activities and water availability by  
53 incorporating GHM with integrated assessment models (Kim et al., 2016).

54           Applying GHMs usually requires miscellaneous inputs, high computation costs, and a  
55 complex calibration process. These challenges stand out in practical situations, especially when  
56 the computation resources are limited. For instance, sensitivity analysis and uncertainty



57 quantification are often needed for decision making, but the users usually cannot afford to run a  
58 large number of simulations with many GHMs like the VIC due to their high computational  
59 expense (Oubeidillah et al., 2014). Another situation is when the users seek reasonable estimates  
60 of water resources with minimal efforts rather than acquiring highly accurate estimates through  
61 expensive inputs of time and efforts. For example, when users seek to explore the  
62 hydroclimatology of a region and its long-term water balance (Sankarasubramanian and Vogel,  
63 2002), then GHMs with fine spatial (e.g., 1/8 degree) and temporal resolution (e.g., hourly) are  
64 not necessarily needed. In this case, GHMs that possess reasonable predictability and are  
65 computationally efficient tend to be more suitable.

66 The motivation of this work arises from the need to construct a hydrological emulator  
67 (HE) that can efficiently mimic the complex GHMs to address the abovementioned issues for  
68 practical use, which provides the opportunity of speeding up simulations at the cost of  
69 introducing some simplification. We develop a HE that is ready-to-use and efficient for any  
70 interested groups or individuals to assess water cycle at basin/regional/global scales. This HE  
71 possesses the following features: 1) minimum number of parameters; 2) minimal climate input  
72 that is easy to acquire; 3) simple model structure; 4) reasonable model fidelity that captures both  
73 the spatial and temporal variability; 5) high computational efficiency; 6) applicable in a range of  
74 spatial scales; and 7) open-source and well-documented.

75 To achieve our goal of identifying a suitable HE, we have explored many hydrological  
76 models to find one that may meet our needs. We then construct the HE based on the “*abcd*”  
77 model out of several reasons: 1) it is widely-used and proved to have reasonable predictability  
78 (Fernandez et al., 2000; Martinez and Gupta, 2010; Sankarasubramanian and Vogel, 2002;  
79 Sankarasubramanian and Vogel, 2003; Thomas, 1981; Vandewiele and Xu, 1992; Vogel and



80 Sankarasubramanian, 2003); 2) it uses a monthly time step and requires less computation cost  
81 than daily or hourly models; 3) it requires minimal inputs; 4) it only involves 4-7 parameters; and  
82 5) it can estimate several variables of interest to a wide range of users (e.g., total runoff,  
83 baseflow, direct runoff, groundwater recharge, evapotranspiration). For the first time we apply  
84 the “*abcd*” based model to the globe, and also for the first time evaluate its predictability and  
85 computational efficiency for both the lumped and distributed schemes, in order to identify a  
86 suitable HE for global applications. Below we describe the model and data in Section 2; and we  
87 present the evaluation of the model, discuss the appropriateness of serving as a HE in Section 3;  
88 finally, in Section 4 we summarize this work with concluding remarks.

89

## 90 **2 Methods and data**

### 91 **2.1 Model description**

92 The monthly “*abcd*” model was first introduced by Thomas (1981) to improve the  
93 national water assessment for the U.S., with a simple analytical framework using only a few  
94 descriptive parameters. It has been widely used across the world, especially for the U.S.  
95 (Martinez and Gupta, 2010; Sankarasubramanian and Vogel, 2002; Sankarasubramanian and  
96 Vogel, 2003). The model uses potential evapotranspiration (PET) and precipitation (P) as input.  
97 The model defines four parameters *a*, *b*, *c*, and *d* that reflect regime characteristics  
98 (Sankarasubramanian and Vogel, 2002; Thomas, 1981) to simulate water fluxes (e.g.,  
99 evapotranspiration, runoff, groundwater recharge) and pools (e.g., soil moisture, groundwater).  
100 The parameters *a* and *b* pertain to runoff characteristics, and *c* and *d* relate to groundwater.  
101 Specifically, the parameter *a* reflects the propensity of runoff to occur before the soil is fully  
102 saturated. The parameter *b* is an upper limit on the sum of evapotranspiration (ET) and soil



103 moisture storage. The parameter  $c$  indicates the degree of recharge to groundwater and is related  
104 to the fraction of mean runoff that arises from groundwater discharge. The parameter  $d$  is the  
105 release rate of groundwater to baseflow, and thus the reciprocal of  $d$  is the groundwater residence  
106 time. Snow is not part of the original “abcd” model, which may result in poor performance of the  
107 model in cold regions where snow significantly affects the hydrological cycle. In this study, we  
108 leverage the work of Martinez and Gupta (2010) which added snow processes into the original  
109 “abcd” model, where the snowpack accumulation and snow melt are estimated based on air  
110 temperature.

111 We adopt the “abcd” framework from Martinez and Gupta (2010) in this work (Fig. 1);  
112 meanwhile, we make three modifications. First, instead of involving three snow parameters in  
113 the parameterization process, we adapt parameter values for two of the parameters (i.e.,  
114 temperature threshold above or below which all precipitation falls as rainfall or snow) from  
115 literature (Wen et al., 2013) and only keep a tunable parameter  $m$  – snow melt coefficient ( $0 < m$   
116  $< 1$ ), in order to enhance the model efficiency with as least necessary parameters as possible.  
117 Second, we introduce the baseflow index (BFI) into the parameterization process to improve the  
118 partition of total runoff between the direct runoff and baseflow (see Section 2.2). Third, other  
119 than the lumped scheme as previous studies used, we first explore the values of model  
120 application in distributed scheme with a grid resolution of 0.5 degree. The detailed model  
121 descriptions and equations are presented in the Appendix A, and the descriptions and ranges of  
122 model parameters are listed in Table 1.

123

## 124 **2.2 Model structure**



125 We evaluate predictability and efficiency for both the lumped and distributed “*abcd*”  
126 model schemes, although most previous applications of the model are conducted in a lumped  
127 scheme (Bai et al., 2015; Fernandez et al., 2000; Martinez and Gupta, 2010; Sankarasubramanian  
128 and Vogel, 2002; Sankarasubramanian and Vogel, 2003; Vandewiele and Xu, 1992; Vogel and  
129 Sankarasubramanian, 2003). In the lumped scheme, each of the 235 river basins is lumped as a  
130 single unit, and each of the climate input (see Section 2.3.1) is the lumped average across the  
131 entire basin, and thus all the model outputs are lumped as well. In terms of the distributed one,  
132 however, each 0.5-degree grid cell has its own climate inputs, and likewise, the model outputs  
133 are simulated at the grid-level. Although the two schemes differ in the spatial resolution of their  
134 inputs and outputs, their within-basin parameters are uniform. We use basin-uniform rather than  
135 grid-specific parameters for the distributed scheme for two reasons: 1) to enhance computational  
136 efficiency; and 2) to avoid drastically different parameters for neighboring grid cells that may be  
137 unrealistic. Note that lateral flows between grid cells and basins are not included at this stage.

138

### 139 **2.3 Data**

#### 140 2.3.1 Climate data

141 The climate data needed only involve monthly total precipitation, monthly mean,  
142 maximum and minimum air temperature. The data we use is obtained from WATCH (Weedon et  
143 al., 2011), spanning the period of 1971-2010, and it is 0.5-degree gridded global monthly data.  
144 The climate data is used for model simulation over the global 235 major river basins (Kim et al.,  
145 2016). Additionally, we use the Hargreaves-Samani method (Hargreaves and Samani, 1982) to  
146 estimate potential evapotranspiration (PET), which is a required input for the model and it needs  
147 climate data of mean, maximum and minimum temperatures for the calculation.





148

## 149 2.3.2 Benchmark runoff data

150 In this study, the “*abcd*” model is tested for its ability to emulate the naturalized  
151 hydrological processes of a reference model since the “true” naturalized hydrological processes  
152 are unknown. The “perfect model” approach is well adopted in climate modeling studies where  
153 one model is treated as “observations” while the others are tested for their ability to reproduce  
154 “observations” (Murphy et al., 2004; Tebaldi and Knutti, 2007). Here, we use the process-based  
155 VIC model as the “perfect model”, which was also driven by the WATCH climate forcing. The  
156 simulated daily runoff from the VIC is aggregated to monthly data to be consistent with the  
157 temporal scale of the “*abcd*” model. The VIC runoff product (Hattermann et al., 2017; Leng et  
158 al., 2015) is then used as a benchmark for calibrating and validating the “*abcd*” model due to two  
159 reasons. First, VIC runoff has been evaluated across many regions of the globe and is proved to  
160 be reasonably well (Abdulla et al., 1996; Hattermann et al., 2017; Maurer et al., 2001; Nijssen et  
161 al., 1997; Nijssen et al., 2001b). Second, since we have not involved river routing, reservoir  
162 regulations and upstream water withdrawals in the “*abcd*” model, the simulated monthly runoff  
163 is more representative of “natural conditions”, and as such it tends to be more reasonable to  
164 compare the simulated runoff against the VIC runoff product rather than observed streamflow  
165 data from stream gauges (Dai et al., 2009; Wilkinson et al., 2014).

166 The VIC runoff product also compares well to other products (see Fig. S1, S2), including  
167 the UNH/GRDC runoff product (Fekete and Vorosmarty, 2011; Fekete et al., 2002) and the  
168 global streamflow product (Dai et al., 2009). The scatterplot pattern of the VIC long-term annual  
169 runoff product vs. the streamflow product matches well with that of the UNH/GRDC runoff vs.  
170 the streamflow product (streamflow is transferred to the same unit as runoff via dividing by the



171 basin area). Further, the correlation coefficient of the VIC and the UNH/GRDC long-term annual  
172 runoff is as high as 0.83 across the global 235 basins. This suggests the reasonability of VIC  
173 runoff product, because the UNH/GRDC runoff is calibrated with the GRDC observations. At  
174 the same time, the discrepancies between the VIC runoff products and the streamflow products  
175 (Fig. S2) may be attributed to human activities, such as reservoir regulations and upstream water  
176 withdrawals, have not been embedded in the runoff but are reflected in the streamflow.

177

### 178 **2.3 Model calibration**

179 Typically, most applications of the “*abcd*” model utilize single-objective optimization to  
180 minimize the difference between measured and simulated streamflow (Bai et al., 2015; Martinez  
181 and Gupta, 2010; Sankarasubramanian and Vogel, 2002). While this may lead to a good fit for  
182 simulated total runoff, however, it will possibly result in inappropriate partition of total runoff  
183 between direct runoff and baseflow (see Section 3.1.2). To improve the accuracy of the  
184 simulated total runoff and the partition between direct runoff and baseflow, we introduce the  
185 baseflow index (BFI) into the objective function. On one side, we maximize Kling-Gupta  
186 efficiency (KGE) (Gupta et al., 2009), which is used as a metric to measure the accuracy of the  
187 simulated total runoff relative to the VIC benchmark runoff. The KGE is defined as the  
188 difference of unity and the Euclidian distance (ED) from the ideal point, thus we maximize KGE  
189 through minimizing the ED. The KGE and ED are calculated as follows (Gupta et al., 2009):

$$190 \quad KGE = 1 - ED \quad (1)$$

$$191 \quad ED = \sqrt{(r-1)^2 + (\alpha-1)^2 + (\beta-1)^2} \quad (2)$$

$$192 \quad r = \frac{Cov_{so}}{\sigma_s \cdot \sigma_s} \quad (3)$$



$$193 \quad \alpha = \frac{\sigma_s}{\sigma_o} \quad (4)$$

$$194 \quad \beta = \frac{\mu_s}{\mu_o} \quad (5)$$

195 where  $r$ ,  $\alpha$ ,  $\beta$ , and  $Cov_{so}$  are relative variability, bias, correlation coefficient, and covariance  
196 between the simulated and observed values (here we treat the VIC runoff as the observed),  
197 respectively;  $\mu$  and  $\sigma$  represent the mean and standard deviation (subscript “s” and “o” stand for  
198 simulated and observed values). On the other side, we nudge the simulated BFI towards the  
199 benchmark BFI (here we treat the benchmark BFI as the observed) – the mean BFI of the four  
200 products from (Beck et al., 2013). Then, the objective function is as follows:

$$201 \quad \min(ED + abs(BFI_{obs} - BFI_{sim}))$$

202 where *min* stands for minimizing the value in the parenthesis, *abs* represents absolute value, ED  
203 is the Euclidian distance between the simulated and observed total runoff (Gupta et al., 2009),  
204  $BFI_{obs}$  and  $BFI_{sim}$  are the observed and simulated BFI, respectively. Here we treat the benchmark  
205 runoff from the VIC and BFI from Beck et al. (2013) as observed values. We then minimize the  
206 objective function for parameter optimization by utilizing a Genetic Algorithm (GA) routine  
207 (Deb et al., 2002). Note that for the distributed model scheme, we aggregate the grid-level total  
208 runoff estimates to basin-level and then nudge it toward basin-level benchmark total runoff  
209 during the calibration process.

210

## 211 **2.4 Model simulations**

212 To evaluate the predictability and efficiency of the “*abcd*” model as a HE, we have  
213 conducted 2 sets of model simulations across the global 235 basins, with one set for calibration  
214 and the other one for validation, for both the lumped and distributed model schemes. For the first



215 set, we run the model for each basin for the period of 1971-1990 to get basin-specific parameters  
216 by using the GA approach (see Section 2.2). For the second set, using the parameters identified  
217 in the first set of simulation, we run the model for the period of 1991-2010 to validate the model  
218 predictability and also evaluate the computational efficiency. Model inputs and outputs in the  
219 distributed scheme are at a spatial resolution of 0.5-degree, whereas those in the lumped scheme  
220 are all in lumped single unit for each basin. All model simulations are conducted in a monthly  
221 time step. Note that broad users can run the model for global 235 basins, or for as many basins as  
222 they want for either scheme, as all the related basin-specific input data and calibrated parameters  
223 for both schemes are open-source.

224

### 225 **3 Results and discussions**

#### 226 **3.1 Evaluation of model predictability**

227 In terms of total runoff, we find the lumped and distributed schemes are comparably  
228 capable in simulating long-term mean annual quantity, temporal variations and spatial patterns  
229 for the vast majority of river basins globally (Fig. 2-4). Estimates of long-term mean annual total  
230 runoff from both the lumped and distributed schemes match very well with that of VIC total  
231 runoff across the 235 basins, with a correlation coefficient ( $r$ ) of higher than 0.96, for both the  
232 calibration and validation period (Fig. 2). Similarly, the basin-level estimates of long-term mean  
233 annual direct runoff and baseflow also match well with those of the VIC across the globe, for  
234 both schemes and both periods (Fig. 2). This suggests both schemes possess the capability in  
235 partitioning total runoff. Also, we find introduction of BFI into the objective function has  
236 improved the partition of total runoff between direct runoff and baseflow (Fig. S4). Specifically,  
237 for the case of involving both the total runoff and BFI in the objective function (see Section 2.2),



238 the correlation efficiencies ( $r$ ) between the long-term annual benchmark and modeled direct  
239 runoff and baseflow from the lumped scheme across global basins are 0.97 and 0.96, respectively.  
240 However, for the case of only involving the total runoff in the objective function, the  $r$  values are  
241 0.86 and 0.72, respectively (See Fig. S4).

242 Furthermore, both schemes display good capability in capturing the seasonal signals of  
243 the total runoff (Fig. 3). Meanwhile, although the spatial patterns of annual total runoff from the  
244 lumped scheme present a general match with that of the VIC, it does not reflect the spatial  
245 variations inside a basin that is however captured by the distributed scheme (Fig. 4). Therefore,  
246 the distributed scheme provides overall slightly higher KGE (Fig. 4-5), with a global mean KGE  
247 value of 0.79 as compared to 0.75 for the lumped scheme (Fig. S3).

248 To ensure good model predictability for the major water fluxes, we also evaluate the  
249 modelled ET estimates. The modelled ET compares reasonably well with the VIC ET product as  
250 well as with the mean synthesis of the LandFlux-EVAL ET product (Mueller et al., 2013),  
251 displaying similar spatial variations (Fig. S5). Likewise, the distributed “*abcd*” scheme tends to  
252 have better capability in presenting spatial heterogeneity than the lumped one. Further, the good  
253 predictability of seasonality in runoff as illustrated in Fig. 4 also reflects similar performance for  
254 ET, given the runoff and ET are the two major water fluxes in the water mass balance and the  
255 soil moisture changes are negligible over long-term.

256 The distributed scheme appears to outperform the lumped scheme in term of goodness-  
257 of-fit, especially in some cold (e.g., Arctic, Northern European, Interior Tibet) and in some dry  
258 (e.g., North Africa) regions (Fig. 5). This is possibly because distributed inputs can reflect basin-  
259 level heterogeneity, and thus better capture the characteristic of the hydrological conditions in  
260 those regions. However, both schemes do not perform well in the southern end of the Andes



261 Mountains (Fig. 5). This may be attributed to the complex land surface characteristics in that  
262 mountainous area, which cannot be resolved due to the coarse spatial resolution. Moreover, the  
263 distributed scheme also tends to perform slightly worse in cold regions (Fig. 5), which is  
264 possibly due to lack of representation for permafrost in the model.

265 Previous studies investigating the credibility of lumped and distributed hydrological  
266 models indicate that, in many cases, lumped models perform comparably or just as well as  
267 distributed models (Asadi, 2013; Brirhet and Benaabidate, 2016; Ghavidelfar et al., 2011;  
268 Michaud and Sorooshian, 1994; Oblad et al., 1994; Reed et al., 2004; Refsgaard and Knudsen,  
269 1996; YAO et al., 1998). However, distributed models may have advantages for predicting  
270 runoff in ungauged watersheds (Reed et al., 2004; Refsgaard and Knudsen, 1996), for capturing  
271 spatial distribution of runoff due to heterogeneity in rainfall patterns or in land surface (Downer  
272 et al., 2002; Paudel et al., 2011; YAO et al., 1998), and for predicting flood peaks (Asadi, 2013;  
273 Brirhet and Benaabidate, 2016; Carpenter and Georgakakos, 2006; Krajewski et al., 1991). Our  
274 results on the predictability of lumped and distributed “*abcd*” model are in line with previous  
275 findings in the literature.

276 The good agreement between our modelled water fluxes, including total runoff, direct  
277 runoff, baseflow and ET, and the benchmark products provides confidence in the capability of  
278 both the lumped and distributed schemes in estimating temporal and spatial variations in major  
279 water fluxes across the globe. In addition, to identify a suitable HE, the required computation  
280 cost is another key factor as detailed below.

281

### 282 **3.2 Evaluation of computational efficiency**



283           While the performance of model predictability is comparable for the lumped and  
284 distributed schemes as elucidated above, great disparity exists for runtime of the two schemes  
285 and the VIC model (Table 2). Take the Amazon basin that covers a total number of 1990 0.5-  
286 degree grid cells as an example, it takes 11.05 minutes for model calibration via the GA method  
287 in the distributed scheme but only 0.16 minute for the lumped one. Similar disparity is also found  
288 for model simulation with calibrated parameters, with runtime of 0.03 and 3.20 seconds for a  
289 1000-year simulation of the Amazon basin for the lumped and distributed schemes, respectively.  
290 However, according to the authors' experience, it will take ~1 week for the VIC model to  
291 accomplish the same job, which is far more computationally expensive. In general, the  
292 computational efficiency of the lumped scheme is two orders of magnitudes higher than the  
293 distributed one, although that of the distributed one is still much higher than the VIC (~five  
294 orders of magnitude) and many other GHMs and land surface models (LSMs).

295

### 296 **3.3 Potential application of the model as a hydrological emulator**

297           The good predictability and computational efficiency of both the distributed or lumped  
298 schemes as elucidated in Sections 3.1 and 3.2 suggest its suitability for serving as HEs that can  
299 efficiently emulate complex GHMs (e.g., the VIC or others). The source codes, input data, basin-  
300 specific parameters across the globe for both the lumped and distributed schemes are open-  
301 source and well-documented, which will make the HE ready to use and facilitate their wide and  
302 easy use with minimal efforts.

303           Moreover, the choice of either the distributed or lumped scheme as HE depends on the  
304 user's specific needs. There is a tradeoff between the model predictability and computational  
305 efficiency. While the distributed scheme tends to better capture the spatial heterogeneity of water



306 fluxes and can produce grid-level outputs that lumped scheme cannot, it incurs heavier  
307 computational cost than the lumped scheme. For applications that aim to strike a balance  
308 between predictability and computation cost, such as practical assessment of water resources, or  
309 estimation of water supply for IAMs, or quantification of uncertainty and sensitivity analyses, it  
310 would be reasonable to employ the lumped scheme as a HE. The lumped scheme is especially  
311 advantageous due to its minimal calibration and computational cost, parsimonious efforts for  
312 model implementation, and reasonable fidelity in estimating major water fluxes (e.g., runoff, ET).  
313 For users from the IAM community, the lumped scheme might be sufficiently suitable for their  
314 needs since 1) the lumped scheme operates at the same spatial resolution at which IAMs  
315 typically balance water demands and supplies ( Kim et al., 2016), and 2) the inherent uncertainty  
316 of the lumped scheme is likely comparable or even overshadowed by the intrinsic uncertainty of  
317 IAMs (Kraucunas et al., 2015; O'Neill et al., 2014). Similarly, for users who aim to conduct  
318 uncertainty and sensitivity analyses, the high computational efficiency of the lumped scheme  
319 allow the users to emulate the hydrological model of interest (e.g., GHMs, LSMs) and then run a  
320 large number of simulations to conduct their uncertainty and sensitivity analysis (Scott et al.,  
321 2016). Therefore, the high computational efficiency makes the lumped scheme more appealing  
322 as a HE in these cases. However, if the research questions hinge on the gridded estimates, or  
323 emphasize the spatial heterogeneity of the water fluxes or pools, it would be more desirable to  
324 deploy the distributed scheme as a HE instead.

325         Based upon our open-source HE and the validated basin-specific parameters across the  
326 globe, researchers can easily investigate the variations in water budgets at the  
327 basin/national/regional/global scale of interest, with minimum requirements of input data,  
328 efficient computation performance and reasonable model fidelity. Likewise, researchers can





329 utilize the framework of the HE with any alternative input data, or recalibrate the HE to emulate  
330 any complex GHM or LSM of interest, to meet their own needs.

331

#### 332 **4 Conclusions**

333       Toward addressing the issue that many global hydrological models (GHMs) are  
334 computationally expensive and thus users cannot afford to conduct a large number of simulations  
335 for various tasks, we firstly construct a hydrological emulator (HE) that possesses both  
336 reasonable predictability and computation efficiency for global applications in this work. Built  
337 upon the widely-used “*abcd*” model, we have adopted two snow-related parameters from  
338 literature rather than tuning them for parameter parsimony, and also have improved the partition  
339 of total runoff between the direct runoff and baseflow by introducing baseflow index into the  
340 objective function of the parameter optimization. We then evaluate the appropriateness of the  
341 model serving as an emulator for a complex GHM –VIC, for both the lumped and distributed  
342 model schemes, by examining their predictability and computational efficiency.

343       In general, both distributed and lumped schemes have comparably good capability in  
344 simulating spatial and temporal variations of the water balance components (i.e., total runoff,  
345 direct runoff, baseflow, evapotranspiration). Meanwhile, the distributed scheme has slightly  
346 better performance than the lumped one (e.g., capturing spatial heterogeneity), with mean Kling-  
347 Gupta efficiency of 0.79 vs. 0.75 across global 235 basins, and also it provides grid-level  
348 estimates that the lumped one incapable of. Additionally, the distributed scheme performs better  
349 in extreme climate regimes (e.g., Arctic, North Africa) and Europe. However, the distributed one  
350 incurs two more orders of magnitudes of computation cost than the lumped one. Therefore, the  
351 lumped scheme could be an appropriate HE – reasonable predictability and high computational



352 efficiency. At the same time, the distributed scheme could be a suitable alternative for research  
353 questions that hinge on grid-level spatial heterogeneity. Finally, upon open-sourcing and well-  
354 documentation, the HE is ready to use and it provides researchers an easy way to investigate the  
355 variations in water budgets at any spatial scale of interest (e.g., basin, region or globe), with  
356 minimum requirements of efforts, reasonable model predictability and appealing computational  
357 efficiency.



358 **Code and/or data availability**

359 The code and data are available on the GitHub open-source software site

360 (<https://github.com/JGCRI/hydro-emulator>). The repository includes the source code (written in Matlab),

361 all related data inputs and outputs for global 235 basins, and a Readme file.



362 **Appendix A: Descriptions and equations of the “abcd” model**

363 The *abcd* model was first introduced by (Thomas, 1981), and Martinez and Gupta (Martinez and  
 364 Gupta, 2010) added snow processes into the model. In this work, we adopted the snow scheme in  
 365 Martinez and Gupta (2010):

$$366 \quad Snow_i = \begin{cases} 0 & T^{rain} < T_i^{min} \\ 367 \quad P_i \times \frac{T^{rain} - T_i^{min}}{T^{rain} - T^{snow}} & T^{snow} < T_i^{min} < T^{rain} \\ 368 \quad P_i & T_i^{min} < T^{snow} \end{cases} \quad (1)$$

$$370 \quad SP_i = SP_{i-1} - SNM_i + Snow_i \quad (2)$$

$$371 \quad SNM_i = \begin{cases} 372 \quad 0 & T_i^{min} < T^{snow} \\ 373 \quad (SP_{i-1} + Snow_i) \times m \times \frac{T^{rain} - T_i^{min}}{T^{rain} - T^{snow}} & T^{snow} < T_i^{min} < T^{rain} \\ 374 \quad (SP_{i-1} + Snow_i) \times m & T^{rain} < T_i^{min} \end{cases} \quad (3)$$

376 where  $P_i$ ,  $SP_i$ ,  $SNM_i$  and  $Snow_i$  are total precipitation, snowpack storage, snowmelt and the  
 377 precipitation as snowfall at time step  $i$ , respectively,  $T^{rain}$  (or  $T^{snow}$ ) stands for the temperature threshold  
 378 above (or below) which all precipitation falls as rainfall (or snow), and  $T_i^{min}$  is the minimum temperature  
 379 at time step  $i$ , and the parameter  $m$  is the snowmelt coefficient. Rather than keeping the three parameters  
 380  $T^{rain}$ ,  $T^{snow}$  and  $m$ , we adopt the  $T^{rain}$  value of 2.5 °C and  $T^{snow}$  value of 0.6 °C (Wen et al., 2013) and  
 381 thus only keep one snowmelt-related parameter  $m$  in the model, in order to alleviate the computation load  
 382 during the parameter optimization process.

383



384 The model defines two state variables “available water” and “evapotranspiration opportunity”,  
385 denoted as  $W_i$  and  $Y_i$ , respectively. The  $W_i$  is defined as:

$$386 \quad W_i = SM_{i-1} + Rain_i + SNM_i \quad (4)$$

387 where  $SM_{i-1}$  is soil moisture at the beginning of time step  $i$ ,  $Rain_i$  and  $SNM_i$  are rainfall and snowmelt  
388 during period  $i$ .

389  $Y_i$  stands for the maximum water that can leave the soil as evapotranspiration ( $ET$ ) at period  $i$ , and  
390 it is defined as below:

$$391 \quad Y_i = ET_i + SM_i \quad (5)$$

392 where  $ET_i$  is the actual ET at time period  $i$  and  $SM_i$  is soil moisture at the end of time step  $i$ . Further,  $Y_i$   
393 has a non-linear relationship with  $W_i$  as:

$$394 \quad Y_i = \frac{W_i - b}{2a} - \sqrt{\left(\frac{W_i - b}{2a}\right)^2 - W_i \times b / a} \quad (6)$$

395 where  $a$  and  $b$  are parameters detailed in Section 2.1.

396 Allocation of  $W_i$  between  $ET_i$  and  $SM_i$  is estimated by assuming that the loss of soil moisture by  
397  $ET$  will be proportional to  $PET$  as:

$$398 \quad \frac{dS}{dt} = -PET \times \frac{SM}{b} \quad (7)$$

399 After integrating the above differential equation and assuming  $S_{i-1} = Y_i$ ,  $SM_i$  can be derived as:

$$400 \quad SM_i = Y_i \times \exp\left(-\frac{PET_i}{b}\right) \quad (8)$$

401 Then,  $ET_i$  can be calculated through equation (2).

402 In the model framework,  $W_i - Y_i$  is the sum of the groundwater recharge ( $RE$ ) and direct runoff  
403 ( $Q_d$ ), and the allocation is determined by the parameter  $c$ :

$$404 \quad RE_i = c \times (W_i - Y_i) \quad (9)$$



405  $Q_d = (1 - c) \times (W_i - Y_i)$  (10)

406 The baseflow from the groundwater (*GW*) pool is modeled as:

407  $Q_b = d \times GW_i$  (11)

408 where *d* is a parameter reflecting the release rate of groundwater to baseflow. Then the total runoff ( $Q_t$ ) is

409 the sum of the direct runoff and baseflow:

410  $Q_t = Q_d + Q_b$  (12)

411 The  $GW_i$  is the sum of groundwater storage at the end of last time step and the groundwater recharge

412 minus the baseflow, and  $GW_i$  is derived as:

413  $GW_i = \frac{GW_{i-1} + RE_i}{1 + d}$  (13)

414 Then, all the water fluxes and pools are solved.

415



416 Author contribution

417 Yaling Liu and Mohamad Hejazi designed this work, and all co-authors offered help through discussions.

418 Yaling Liu developed the hydrological emulator and conducted the simulations and evaluations. Yaling

419 Liu wrote the manuscript, and all co-authors contributed to the revision.



420 **Competing interests**

421 The authors declare that they have no conflict of interests.





422 **Acknowledgement:** This research was supported by the Office of Science of the U.S.  
423 Department of Energy through the Integrated Assessment Research Program. PNNL is operated  
424 for DOE by Battelle Memorial Institute under contract DE-AC05-76RL01830.

425 **References**

426

427 Abdulla, F.A., Lettenmaier, D.P., Wood, E.F., Smith, J.A., 1996. Application of a macroscale hydrologic

428 model to estimate the water balance of the Arkansas-Red River Basin. *Journal of Geophysical*  
429 *Research: Atmospheres*, 101(D3): 7449-7459.430 Alcamo, J., Henrichs, T., 2002. Critical regions: A model-based estimation of world water resources  
431 sensitive to global changes. *Aquat. Sci.*, 64(4): 352-362.432 Alkama, R. et al., 2010. Global evaluation of the ISBA-TRIP continental hydrological system. Part I:  
433 Comparison to GRACE terrestrial water storage estimates and in situ river discharges. *J.*  
434 *Hydrometeorol.*, 11(3): 583-600.435 Arnell, N.W., Gosling, S.N., 2013. The impacts of climate change on river flow regimes at the global  
436 scale. *J. Hydrol.*, 486: 351-364.437 Asadi, A., 2013. The Comparison of Lumped and Distributed Models for Estimating Flood Hydrograph  
438 (Study Area: Kabkian Basin). *J. Electron. Commun. Eng. Res.*, 1(2): 7-13.439 Bai, P., Liu, X., Liang, K., Liu, C., 2015. Comparison of performance of twelve monthly water balance  
440 models in different climatic catchments of China. *J. Hydrol.*, 529: 1030-1040.441 Beck, H.E. et al., 2013. Global patterns in base flow index and recession based on streamflow  
442 observations from 3394 catchments. *Water Resour. Res.*, 49(12): 7843-7863.443 Beven, K., Kirkby, M., 1977. Towards a Simple, Physically-based, Variable Contributing Area Model of  
444 Catchment Hydrology. University of Leeds, School of Geography.445 Bierkens, M., Van Beek, L., 2009. Seasonal predictability of European discharge: NAO and hydrological  
446 response time. *J. Hydrometeorol.*, 10(4): 953-968.447 Brirhet, H., Benaabidate, L., 2016. Comparison Of Two Hydrological Models (Lumped And Distributed)  
448 Over A Pilot Area Of The Issen Watershed In The Souss Basin, Morocco. *European Scientific*  
449 *Journal*, 12(18).450 Burnash, R.J., Ferral, R.L., McGuire, R.A., 1973. A generalized streamflow simulation system,  
451 conceptual modeling for digital computers, U.S. Department of Commerce, National Weather  
452 Service, and State of California, Department of Water Resources, Sacramento, CA.453 Carpenter, T.M., Georgakakos, K.P., 2006. Intercomparison of lumped versus distributed hydrologic  
454 model ensemble simulations on operational forecast scales. *J. Hydrol.*, 329(1): 174-185.455 Dai, A., Qian, T., Trenberth, K.E., Milliman, J.D., 2009. Changes in continental freshwater discharge  
456 from 1948 to 2004. *J. Clim.*, 22(10): 2773-2792.457 De Graaf, I., Van Beek, L., Wada, Y., Bierkens, M., 2014. Dynamic attribution of global water demand to  
458 surface water and groundwater resources: Effects of abstractions and return flows on river  
459 discharges. *Advances in Water Resources*, 64: 21-33.460 Deb, K., Pratap, A., Agarwal, S., Meyarivan, T., 2002. A fast and elitist multiobjective genetic algorithm:  
461 NSGA-II. *IEEE transactions on evolutionary computation*, 6(2): 182-197.462 Döll, P., Fiedler, K., Zhang, J., 2009. Global-scale analysis of river flow alterations due to water  
463 withdrawals and reservoirs. *Hydrology and Earth System Sciences*, 13(12): 2413-2432.464 Downer, C.W., Ogden, F.L., Martin, W.D., Harmon, R.S., 2002. Theory, development, and applicability  
465 of the surface water hydrologic model CASC2D. *Hydrol. Processes*, 16(2): 255-275.466 Edmonds, J. et al., 1997. An integrated assessment of climate change and the accelerated introduction of  
467 advanced energy technologies—an application of MiniCAM 1.0. *Mitigation and adaptation*  
468 *strategies for global change*, 1(4): 311-339.469 Fekete, B., Vorosmarty, C., 2011. ISLSCP II UNH/GRDC Composite Monthly Runoff. ISLSCP Initiative  
470 II Collection, edited by: Hall, FG, Collatz, G., Meeson, B., Los, S., Brown de Colstoun, E., and  
471 Landis, D., Data set, available at: <http://daac.ornl.gov/>, from Oak Ridge National Laboratory  
472 Distributed Active Archive Center, Oak Ridge, Tennessee, USA, doi, 10.473 Fekete, B.M., Vörösmarty, C.J., Grabs, W., 2002. High-resolution fields of global runoff combining  
474 observed river discharge and simulated water balances. *Global Biogeochem. Cycles*, 16(3).



- 475 Fernandez, W., Vogel, R., Sankarasubramanian, A., 2000. Regional calibration of a watershed model.  
476 Hydrol. Sci. J., 45(5): 689-707.
- 477 Gerten, D. et al., 2005. Contemporary “green” water flows: Simulations with a dynamic global vegetation  
478 and water balance model. Physics and Chemistry of the Earth, Parts A/B/C, 30(6): 334-338.
- 479 Ghavidelfar, S., Alvankar, S.R., Razmkhah, A., 2011. Comparison of the lumped and quasi-distributed  
480 Clark runoff models in simulating flood hydrographs on a semi-arid watershed. Water Resour.  
481 Manage., 25(6): 1775-1790.
- 482 Gupta, H.V., Kling, H., Yilmaz, K.K., Martinez, G.F., 2009. Decomposition of the mean squared error  
483 and NSE performance criteria: Implications for improving hydrological modelling. J. Hydrol.,  
484 377(1): 80-91.
- 485 Hanasaki, N. et al., 2008. An integrated model for the assessment of global water resources–Part 2:  
486 Applications and assessments. Hydrology and Earth System Sciences, 12(4): 1027-1037.
- 487 Hargreaves, G.H., Samani, Z.A., 1982. Estimating potential evapotranspiration. Journal of the Irrigation  
488 and Drainage Division, 108(3): 225-230.
- 489 Hattermann, F. et al., 2017. Cross-scale intercomparison of climate change impacts simulated by regional  
490 and global hydrological models in eleven large river basins. Clim. Change: 1-16.
- 491 Kim, S.H., Edmonds, J., Lurz, J., Smith, S.J., Wise, M., 2006. The O bj ECTS framework for integrated  
492 assessment: Hybrid modeling of transportation. The Energy Journal: 63-91.
- 493 Kim, S.H. et al., 2016. Balancing global water availability and use at basin scale in an integrated  
494 assessment model. Clim. Change, 136(2): 217-231.
- 495 Krajewski, W.F., Lakshmi, V., Georgakakos, K.P., Jain, S.C., 1991. A Monte Carlo study of rainfall  
496 sampling effect on a distributed catchment model. Water Resour. Res., 27(1): 119-128.
- 497 Kraucunas, I. et al., 2015. Investigating the nexus of climate, energy, water, and land at decision-relevant  
498 scales: the Platform for Regional Integrated Modeling and Analysis (PRIMA). Clim. Change,  
499 129(3-4): 573-588.
- 500 Leng, G., Tang, Q., Rayburg, S., 2015. Climate change impacts on meteorological, agricultural and  
501 hydrological droughts in China. Global Planet. Change, 126: 23-34.
- 502 Liang, X., Lettenmaier, D.P., Wood, E.F., Burges, S.J., 1994. A simple hydrologically based model of  
503 land surface water and energy fluxes for general circulation models. J. Geophys. Res. [Atmos.],  
504 99(D7): 14415-14428.
- 505 Liu, Y. et al., 2015. Agriculture intensifies soil moisture decline in Northern China. Scientific reports, 5:  
506 11261.
- 507 Liu, Y. et al., 2013. Response of evapotranspiration and water availability to changing climate and land  
508 cover on the Mongolian Plateau during the 21st century. Global Planet. Change, 108: 85-99.
- 509 Liu, Y. et al., 2014. Response of evapotranspiration and water availability to the changing climate in  
510 Northern Eurasia. Clim. Change, 126(3-4): 413-427.
- 511 Martinez, G.F., Gupta, H.V., 2010. Toward improved identification of hydrological models: A diagnostic  
512 evaluation of the “abcd” monthly water balance model for the conterminous United States. Water  
513 Resour. Res., 46(8).
- 514 Maurer, E.P., O'Donnell, G.M., Lettenmaier, D.P., Roads, J.O., 2001. Evaluation of the land surface water  
515 budget in NCEP/NCAR and NCEP/DOE reanalyses using an off-line hydrologic model. Journal  
516 of Geophysical Research: Atmospheres, 106(D16): 17841-17862.
- 517 Michaud, J., Sorooshian, S., 1994. Comparison of simple versus complex distributed runoff models on a  
518 mid-sized semiarid watershed. Water Resour. Res., 30(3): 593-605.
- 519 Mueller, B. et al., 2013. Benchmark products for land evapotranspiration: LandFlux-EVAL multi-data set  
520 synthesis. Hydrology and Earth System Sciences.
- 521 Murphy, J.M. et al., 2004. Quantification of modelling uncertainties in a large ensemble of climate  
522 change simulations. Nature, 430(7001): 768-772.



- 523 Nijssen, B., Lettenmaier, D.P., Liang, X., Wetzel, S.W., Wood, E.F., 1997. Streamflow simulation for  
524 continental-scale river basins. *Water Resour. Res.*, 33(4): 711-724.
- 525 Nijssen, B., O'donnell, G.M., Hamlet, A.F., Lettenmaier, D.P., 2001a. Hydrologic sensitivity of global  
526 rivers to climate change. *Clim. Change*, 50(1-2): 143-175.
- 527 Nijssen, B., O'Donnell, G.M., Lettenmaier, D.P., Lohmann, D., Wood, E.F., 2001b. Predicting the  
528 discharge of global rivers. *J. Clim.*, 14(15): 3307-3323.
- 529 O'Neill, B.C. et al., 2014. A new scenario framework for climate change research: the concept of shared  
530 socioeconomic pathways. *Clim. Change*, 122(3): 387-400.
- 531 Obled, C., Wendling, J., Beven, K., 1994. The sensitivity of hydrological models to spatial rainfall  
532 patterns: an evaluation using observed data. *J. Hydrol.*, 159(1-4): 305-333.
- 533 Oubeidillah, A.A., Kao, S.-C., Ashfaq, M., Naz, B.S., Tootle, G., 2014. A large-scale, high-resolution  
534 hydrological model parameter data set for climate change impact assessment for the conterminous  
535 US. *Hydrology and Earth System Sciences*, 18(1): 67-84.
- 536 Paudel, M., Nelson, E.J., Downer, C.W., Hotchkiss, R., 2011. Comparing the capability of distributed and  
537 lumped hydrologic models for analyzing the effects of land use change. *Journal of*  
538 *Hydroinformatics*, 13(3): 461-473.
- 539 Reed, S. et al., 2004. Overall distributed model intercomparison project results. *J. Hydrol.*, 298(1): 27-60.
- 540 Refsgaard, J.C., Knudsen, J., 1996. Operational validation and intercomparison of different types of  
541 hydrological models. *Water Resour. Res.*, 32(7): 2189-2202.
- 542 Rost, S., Gerten, D., Heyder, U., 2008. Human alterations of the terrestrial water cycle through land  
543 management. *Advances in Geosciences*, 18: 43-50.
- 544 Sankarasubramanian, A., Vogel, R.M., 2002. Annual hydroclimatology of the United States. *Water*  
545 *Resour. Res.*, 38(6).
- 546 Sankarasubramanian, A., Vogel, R.M., 2003. Hydroclimatology of the continental United States.  
547 *Geophys. Res. Lett.*, 30(7).
- 548 Scott, M.J. et al., 2016. Sensitivity of future US Water shortages to socioeconomic and climate drivers: a  
549 case study in Georgia using an integrated human-earth system modeling framework. *Clim.*  
550 *Change*, 136(2): 233-246.
- 551 Tang, Q. et al., 2010. Dynamics of terrestrial water storage change from satellite and surface observations  
552 and modeling. *J. Hydrometeorol.*, 11(1): 156-170.
- 553 Tebaldi, C., Knutti, R., 2007. The use of the multi-model ensemble in probabilistic climate projections.  
554 *Philosophical Transactions of the Royal Society of London A: Mathematical, Physical and*  
555 *Engineering Sciences*, 365(1857): 2053-2075.
- 556 Thomas, H., 1981. Improved methods for national water assessment. Report WR15249270, US Water  
557 Resource Council, Washington, DC.
- 558 Van Beek, L., Bierkens, M.F., 2009. The global hydrological model PCR-GLOBWB: conceptualization,  
559 parameterization and verification. Utrecht University, Utrecht, The Netherlands.
- 560 Vandewiele, G., Xu, C.-Y., 1992. Methodology and comparative study of monthly water balance models  
561 in Belgium, China and Burma. *J. Hydrol.*, 134(1-4): 315-347.
- 562 Vogel, R.M., Sankarasubramanian, A., 2003. Validation of a watershed model without calibration. *Water*  
563 *Resour. Res.*, 39(10).
- 564 Vörösmarty, C.J., Green, P., Salisbury, J., Lammers, R.B., 2000. Global water resources: vulnerability  
565 from climate change and population growth. *science*, 289(5477): 284-288.
- 566 Weedon, G. et al., 2011. Creation of the WATCH forcing data and its use to assess global and regional  
567 reference crop evaporation over land during the twentieth century. *J. Hydrometeorol.*, 12(5): 823-  
568 848.
- 569 Wen, L., Nagabhatla, N., Lü, S., Wang, S.-Y., 2013. Impact of rain snow threshold temperature on snow  
570 depth simulation in land surface and regional atmospheric models. *Adv. Atmos. Sci.*, 30(5):  
571 1449-1460.



- 572 Widén-Nilsson, E., Halldin, S., Xu, C.-y., 2007. Global water-balance modelling with WASMOD-M:  
573 Parameter estimation and regionalisation. *J. Hydrol.*, 340(1): 105-118.
- 574 Wilkinson, K., von Zubern, M., Scherzer, J., 2014. Global Freshwater Fluxes into the World Oceans,  
575 Tech. Report prepared for the GRDC.-Koblenz, Federal Institute of Hydrology (BfG),(GRDC  
576 Report No. 44. doi: 10.5675/GRDC\_Report\_44, 23pp.[Available from [http://www. bafg.  
577 de/GRDC/EN/02\\_srvcs/24\\_rprtrs/report\\_44. pdf](http://www.bafg.de/GRDC/EN/02_srvcs/24_rprtrs/report_44.pdf)].
- 578 YAO, H., HASHINO, M., TERAOKAWA, A., SUZUKI, T., 1998. Comparison of distributed and lumped  
579 hydrological models. *PROCEEDINGS OF HYDRAULIC ENGINEERING*, 42: 163-168.
- 580



581 **Figure Caption**

582 **Figure 1** Schematic diagram of the “*abcd*” model, with enhancements of snow and partition of  
583 total runoff between direct runoff and baseflow.

584 **Figure 2** Comparison of basin-specific long-term annual total runoff, direct runoff and baseflow  
585 estimates from both the lumped and distributed “*abcd*” model schemes against VIC products,  
586 across global 235 basins and for the calibration period of 1971-1990 and validation period of  
587 1991-2010. The labels are denoted as combination of model scheme and period, where lump and  
588 dist stand for lumped and distributed model scheme, cal and val represent the calibration and  
589 validation period, respectively. These denotations remain the same for all figures in this work.  
590 Note that the basin-level VIC baseflow is derived by multiplying the gridded VIC long-term  
591 annual total runoff and the mean of the four gridded baseflow index products from Beck et al.  
592 (2014), and then aggregating from grid-level to basin-level. The basin-level VIC direct runoff is  
593 then calculated by subtracting baseflow from the total runoff.

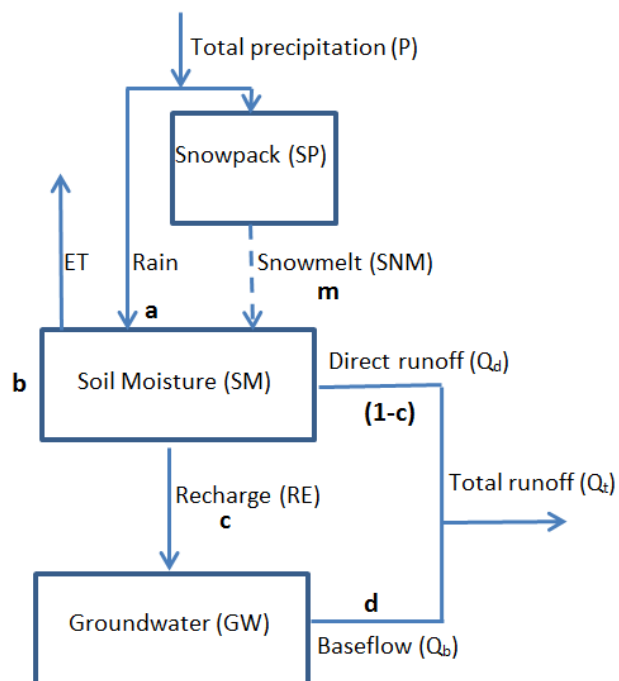
594 **Figure 3** Time series of basin-specific total runoff ( $Q_{\text{total}}$ ) from the VIC product, the lumped and  
595 distributed “*abcd*” schemes for the world’s sixteen river basins with top annual flow (Dai et al.  
596 2009) during 1981-1990.  $KGE_l$  and  $KGE_d$  stand for KGE value for the lumped and distributed  
597 scheme, respectively.

598 **Figure 4** Spatial patterns of long-term annual total runoff ( $\text{mm yr}^{-1}$ ) across global 235 basins: a)  
599 VIC runoff product; b) total runoff estimates from the lumped “*abcd*” scheme (lump = lumped);  
600 and c) total runoff estimates from the distributed “*abcd*” scheme (dist = distributed).

601 **Figure 5** The spatial pattern of Kling-Gupta efficiency (KGE) for the total runoff estimates of  
602 the global 235 basins for the calibration period of 1971-1990: a) the lumped “*abcd*” scheme; and  
603 b) the distributed “*abcd*” scheme.



604 Figure 1

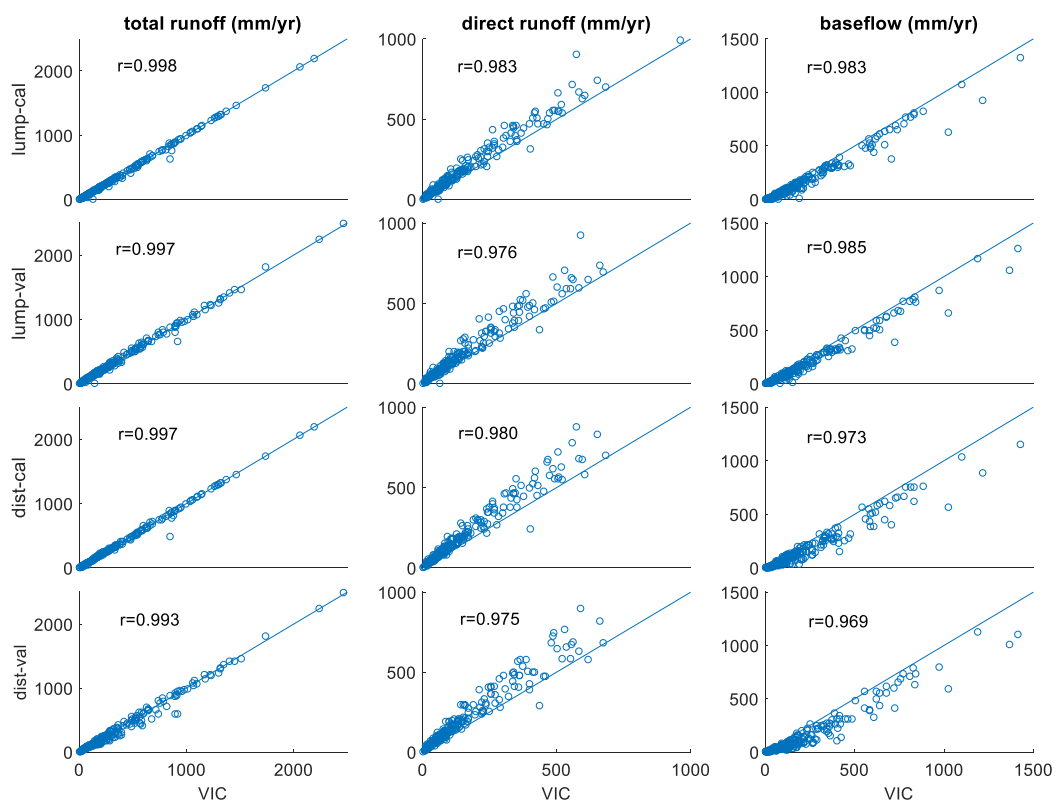


605

606



607 Figure 2



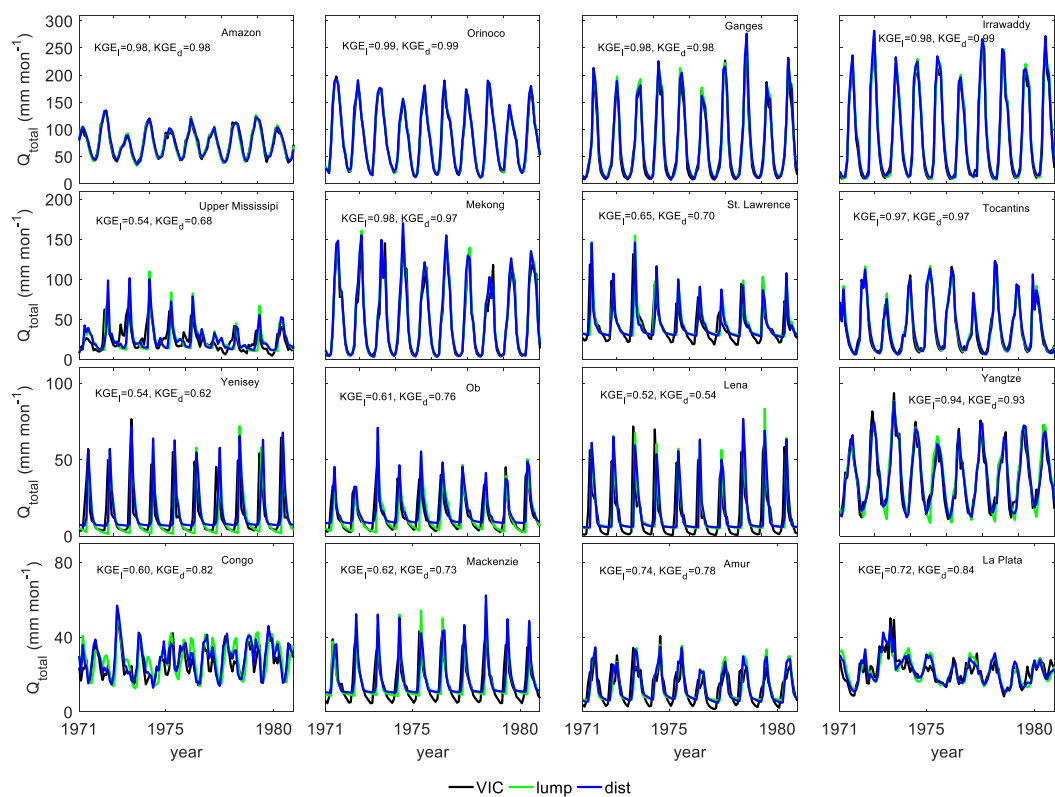
608

609





610 Figure 3

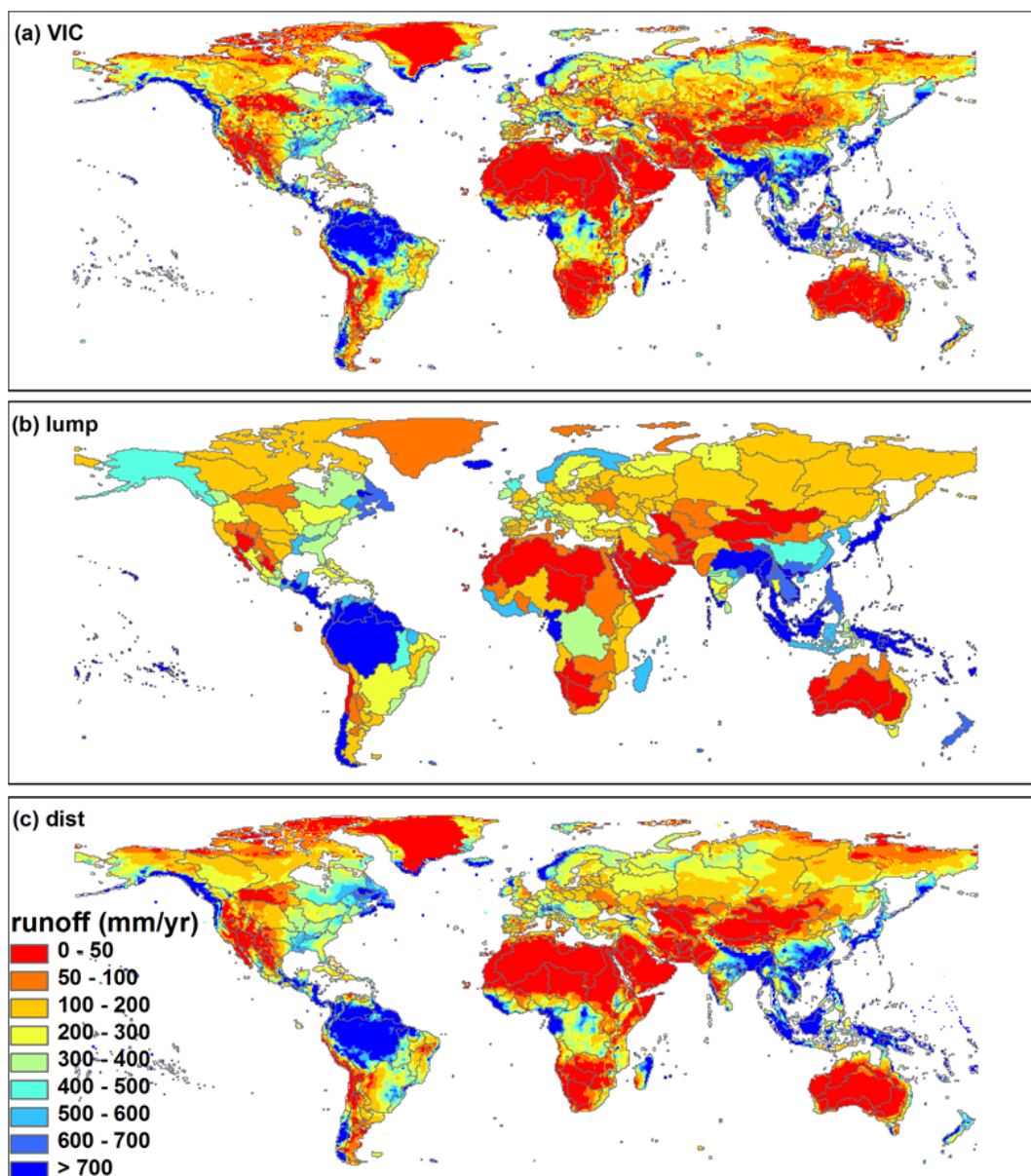


611

612



613 Figure 4

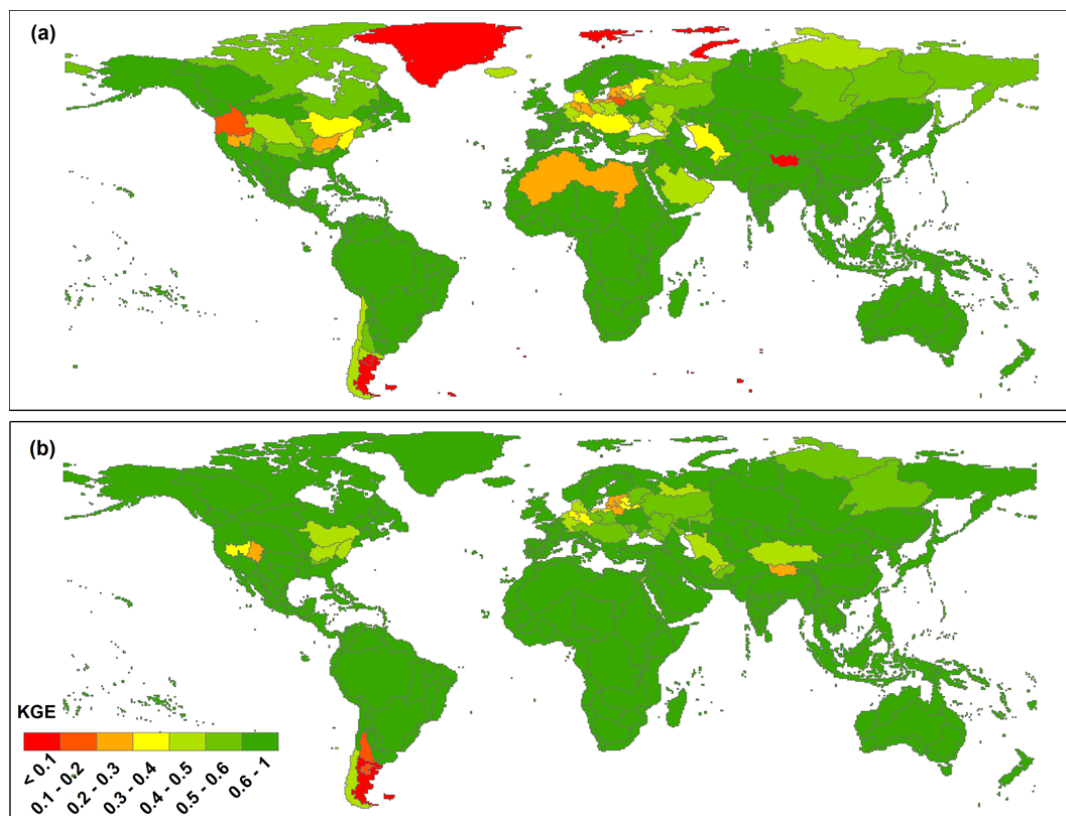


614

615



616 Figure 5



617



618 Table 1 Parameters description and ranges for the “*abcd*” model (the parameters *a, c, d* and *m* are  
619 dimensionless, and the unit for parameter *b* is mm)

<b>parameter</b>	<b>description</b>	<b>range</b>	<b>references</b>
<i>a</i>	Propensity of runoff to occur before the soil is fully saturated	0-1	(Alley, 1984; Martinez and Gupta, 2010;
<i>b</i>	Upper limit on the sum of evapotranspiration and soil moisture storage	0-4000	Sankarasubramanian and Vogel, 2002;
<i>c</i>	Degree of recharge to groundwater	0-1	Vandewiele and Xu,
<i>d</i>	Release rate of groundwater to baseflow	0-1	1992)
<i>m</i>	Snow melt coefficient	0-1	(Wen et al., 2013)

620

621



622 Table 2 Runtime for model calibration and simulation at Amazon basin for the lumped (lump)  
623 and distributed (dist) “abcd” model scheme, as well as for the VIC model.

	<b>calibration</b>	<b>1000 years' simulation</b>
<b>lump</b>	0.16 min	0.03 s
<b>dist</b>	11.05 min	3.20 s
<b>VIC</b>	N/A	~ 1 week

624